Vulnerability Assessment of Tsunami-Affected Inundated Area Using Geospatial Analysis Based Tsunami Run-Up Simulation

by Lusmeilia Afriani

Submission date: 28-Jan-2022 02:11PM (UTC+0700)
Submission ID: 1749846810
File name: ea_Using_Geospatial_Analysis_Based_Tsunami_Run-Up_Simulation.pdf (1.68M)
Word count: 5609
Character count: 29307

Vulnerability Assessment of Tsunami-Affected Inundated Area Using Geospatial Analysis Based Tsunami Run-Up Simulation

Rina Febrina[1*], Lusmelia Afriani[2], Rr M I Retno Susilorini[3] and Tri Prastio[1]
[1]Departement of Civil Engineering, Universitas Malahayati, Bandar Lampung 35153, Indonesia
[2]Departement of Civil Engineering, Universitas Lampung, Bandar Lampung 35153, Indonesia
[3]Departement of Infrastucture and Environmental Engineering, Soegijapranata Catholic University, Semarang 5023, Indonesia

*Corresponding e-mail: febrinacivil@yahoo.com

Abstract. A tsunami can cause considerable loss of life, extreme property damage and infrastructure destruction. A tsunami run-up simulation can be used to forecast wave generation caused by an earthquake. This study aims to assess the tsunami-affected inundated area on the west coast of Lampung province using geospatial analysis-based tsunami run-up simulation. The parameters used in the assessment were applied elevation and slope computed from Aster GDEM, coastline distance determined from a vector map and tsunami inundation obtained by Hills and Mader equation and vegetation density calculated from ALOS ANVIR-2 image. The AHP process was applied for weighing the parameter through a pair-wise comparison using four iterations of the normalised matrix. Five classes of vulnerability were defined and analysed for the tsunami inundation mapping. Weighted overlay through spatial analyst in GIS was used to draw the final map of tsunami vulnerability. The assessment result indicates that 11.26 square kilometre of the study area falls under the high tsunami vulnerability zone and 6.6 square kilometres of the building area comes under the inundation area. The results presented in this study may facilitate improvements in basic data for city planning related to evacuation processes and management strategies during disasters.

Keywords: tsunami, property damage, infrastructure, vulnerability

1. Introduction

Tsunami based disasters are natural, highly destructive and unavoidable phenomena. Vulnerability mapping assessments of a tsunami are observed as an effective way of reducing the impact of the disasters and have been successfully applied for disaster mitigation measures [1-4]. The assessments include the mapping of evacuation covering routes and buildings, the construction of tsunami barriers, disaster risk management and regulation and disaster education for the public [5]. Several pieces of formative information such as reliable and accurate spatial and temporal characteristics and impact of a tsunami with damage potential at different magnitude scales are required for the assessments. The availability of the information has created more parameters which are vitally important in developing a realistic description of vulnerability for a spatial and temporal assessment. The probability of risk, exposure, capacity measurement, and vulnerability are parameters used to determine a disaster risk [6-8]. However, it was shown that external pressure imperilled a person, community, or a system. Vulnerability is explained as a process and condition refers to that produced by economic,

environmental, physical, and social factors. Moreover, vulnerability enhanced the susceptibility of hazards impact community [9,10].

Mapping the distribution of damage area because of disasters and assessing the vulnerability area via remote sensing and GIS are seen to be a potentially effective way of mitigating the disastrous impact of a tsunami. Geo-reference data were used to make a decision, while GIS analysis was employed for the assessment through spatial multi-criteria. On top of that, geographical references and criterion attributes were needed [11,12]. Previous studies used the GIS method for tsunami and an overlay of official land-use mapping [13]. In addition, while GIS can be used to analyse the risk of tsunami, remote sensing data and analysis of the physical built-up of infrastructures, such as building, contour of inundation area, and highest level of tsunami can be used to predict vulnerability [5],[14].

The aims of this study are to map tsunami vulnerability areas on the west coast of Lampung Province and to evaluate the tsunami impact by mapping possible inundation areas using a geospatial analysis-based tsunami run-up simulation. Vulnerability is calculated based on the run-up, elevation, slope, coastline distance and vegetation density using tsunami run-up simulation generated by software L-2008. Furthermore, the Soil Adjusted Vegetation Index (SAVI) is applied. The vegetation mapping is used as a Normalised Difference Vegetation Index (NDVI). In addition, the analytical hierarchy process is used to estimate the weights of the parameters.

2. Research Methodology

2.1. Data

The ASTER Global Digital Elevation Model (ASTER GDEM) version 2 provided the elevation data. ASTER GDEM was used as a platform for data collection via a space-borne observing optical device, while the 2nd version of ASTER GDEM was used to enhance the resolution of global digital elevation and the accuracy of elevation. In addition, ASTER GDEM was also used in advancing algorithm and reprocessing a total of 1.5 million scene data, including 250,000 additional scenes acquired after the previous release. The data were posted approximately 30 m at the equator. Subsequently, the ALOS ANVIR-2 image was analysed for the vegetation density mapping. Moreover, run-up information was used based on the tsunami run-up simulation (L-2008). The protocols of analysis were started from the data collection itself. It proceeded with the surface analysis of DEM data, vector data processing, and inundation processing which continued with the AHP process and finally the raster overlay processing through the GIS approach as in Figure 1.

2.2. Study area

The study was conducted on the west coast of Lampung Province as in Figure 2, non the island of Sumatra. It is an area which is highly exposed to a wide range of potentially devastating impacts from earthquake and tsunami threats.

2.3. Simulation of tsunami

2.3.1. Source modelling

The initial profile of a tsunami centre can be obtained by considering it as a seabed deformation with fault parameters, determined on the mechanism solution data of an earthquake centre. The parameter setting for the source modelling is shown in Figure 3. A11 (km) and A12 (km) refer to the fault length, and Aw1 is the fault width. The positions x_eq fault, y_eq, and z_eq are defined as the longitude, latitude and depth of the earthquake, respectively. Furthermore, the source modelling was conducted using the L-2008 software. The output of the source modelling is the vertical displacement that occurs in the seabed. Subsequently, this deformation was used in the ocean and run-up modelling.

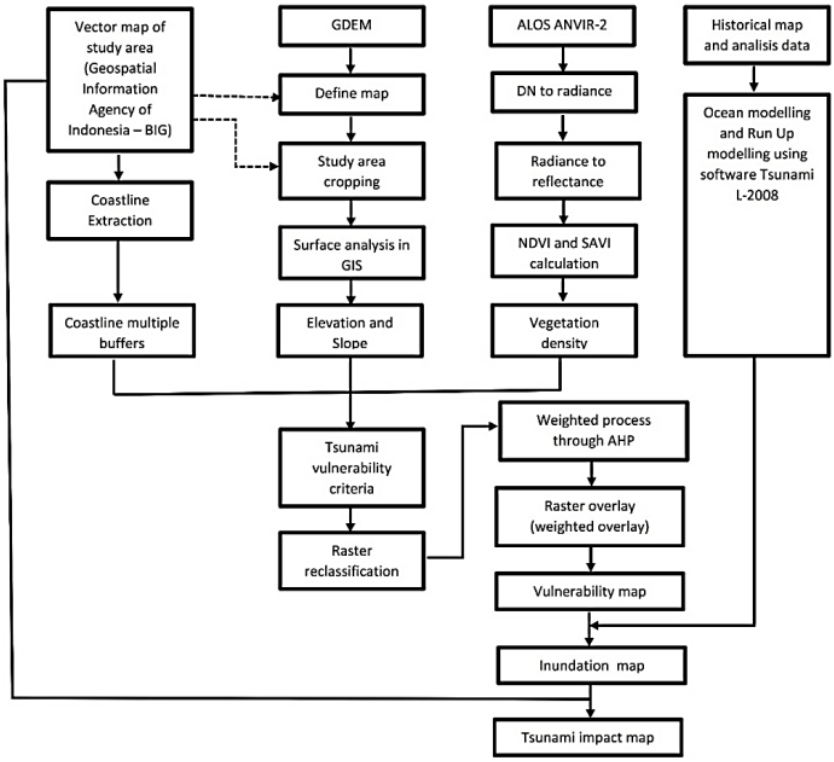

Figure 1. General framework of study

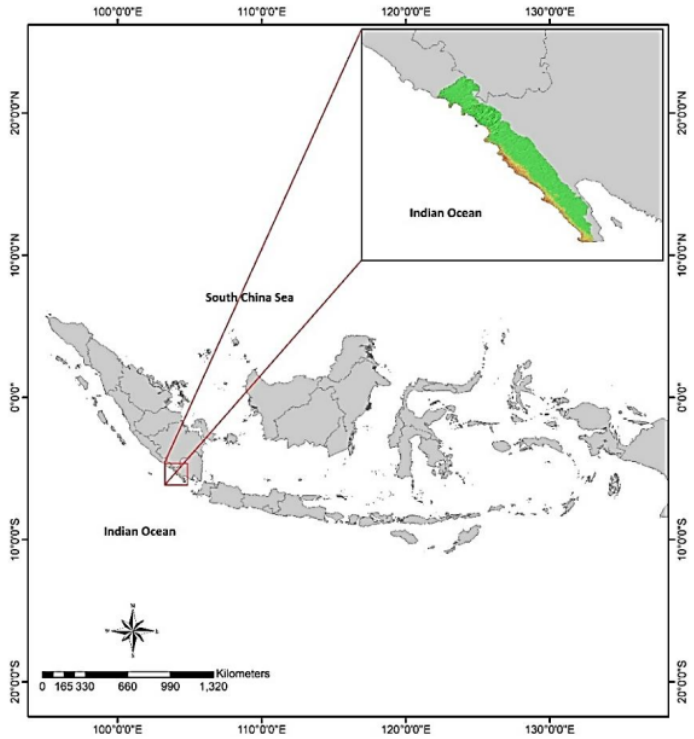

Figure 2. Map of study area

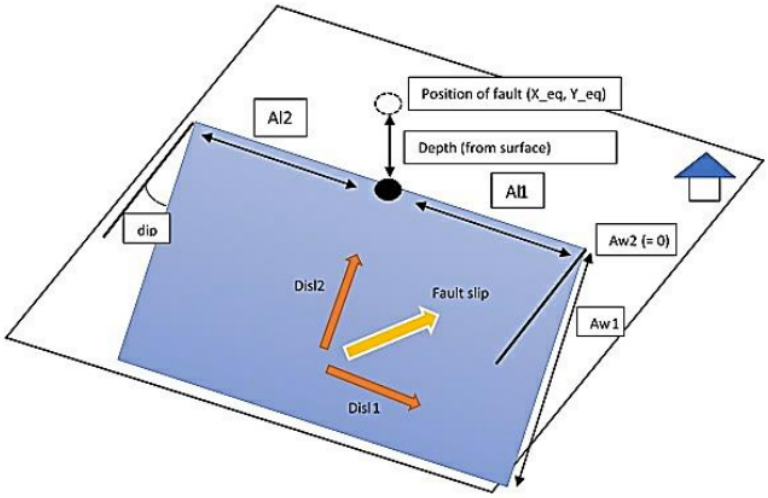

Figure 3. Parameter setting for source modelling

2.3.2. Ocean modelling

Output data of source modelling and bathymetric data were needed for ocean modelling. In addition, the appropriate bathymetric data with a study area was needed to get a good simulation result. In this ocean modelling, the parameter simulation as an input software tsunami L-2008 was maximum time. Maximum time was needed to vine the simulation of 3600s. Subsequently, the data save internal of 25s was added and resulted in 1 output per 25s.

2.3.3. Run-up Modelling

In this study, the height of the tsunami modelling (run-up modelling) was demonstrated by digitising the predetermined area. Digitising was conducted at various points along the coastline of the tsunami-affected area. On observation, every affected area recorded the highest run-up value.

2.4. Spatial analysis

2.4.1. Elevation classification

Elevation data are required to calculate vulnerability and tsunami inundation. A digital elevation model was created using an elevation map. The data from GDEM which were downloaded from DEMNAS website were used to derive a set of physical vulnerability parameters. The elevation was then classified into five vulnerability categories as in Figure 4 based on the height of the surface. A low elevation for example indicated a high tsunami vulnerability wave as in Table 1.

Table 1. Vulnerability class based on elevation, slope and coastline distance [15], [16]

Elevation (m)	Slope (%)	Coastline distance (m)	Vulnerability class
< 5	0 – 2	0-545.65	High
5 - 10	2 – 6	545.65 - 1261.80	Slightly high
10 - 15	6 – 13	1261.80 - 2187.40	Medium
15 - 20	13 – 20	2187.40 - 3154.65	Slightly low
>20	>20	>3154.65	Low

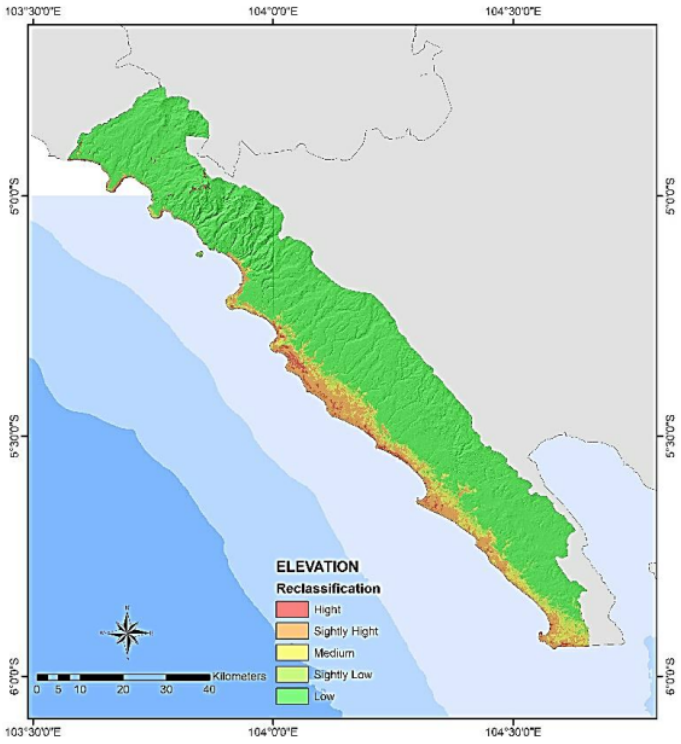

Figure 4. Tsunami vulnerability map based on parameters of elevation

2.4.2. Slope

In this study, a slope is identified based on the maximum changing of the z-value rate from each cell of the image. The third-order finite difference method and GDEM were applied to create a slope map. The range of the slope percentage was identified as zero to almost infinity. The slope map was categorised into five categories according to the value of tsunami vulnerability, as described in Table 1. The vulnerability map shown in Figure. 5 was made by applying slope classification, which is based on the tsunami vulnerability class.

2.4.3. Coastline distance

Coastal areas were divided into five classes of vulnerability using a multi-buffering calculation. Buffering distance was determined using the possibility range of tsunami when reaching the ground. The maximum tsunami height which was obtained from historical reports was used to calculate the buffering distance below [13],[17]:

$$logX_{max} = \log 100 + \frac{4}{3} log \left(\frac{Y_0}{10}\right) \quad (1)$$

where X_{max} is the maximum reach of the tsunami over land, and $Y_o$is the tsunami height at the coast. Besides, the buffering distance was determined based on the range of possible tsunami flows flowing

toward the inland. The score of the X_{max} in this study was based on the simulation of a tsunami using software L-2008. Coastline distances in the vector map of Lampung through GIS processing were used to generate a vulnerability map based on coastline distance.

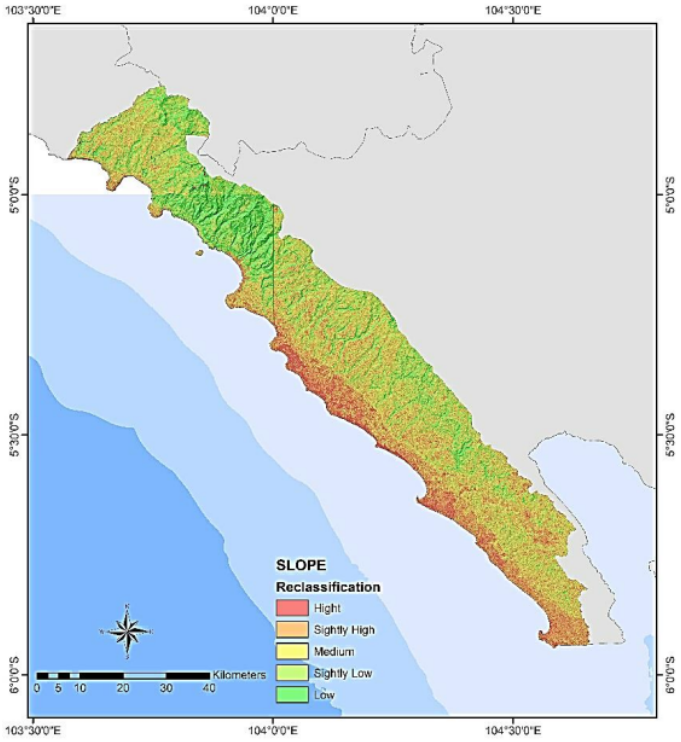

Figure 5. Tsunami vulnerability map based on parameters of slope

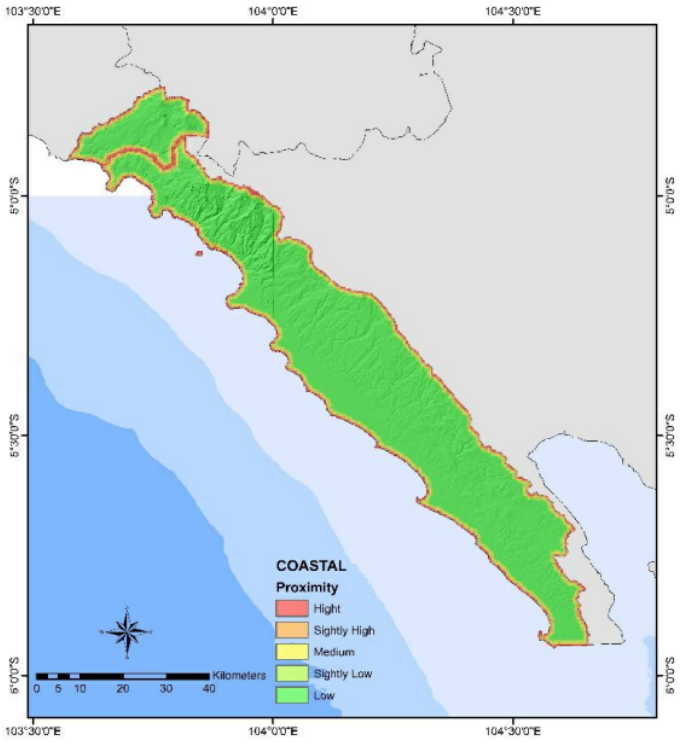

Figure 6. Tsunami vulnerability map based on the parameters of coastline distance

2.4.4. Inundation

The simulation of a tsunami was demonstrated using ArcGIS 10.6 software with the Raster calculator functions [21] as shown below:

$$X_{max} = (Hs)^{1,33} n^{-2}\ k\ Cos\ S \quad (2)$$

where X_{max} is the maximum inundation (m), Hs is the maximum tsunami run-up (m), $k$is constant (0.06), manning coefficient of the land is n, the slope of the land is S, and X_{max} in the vector map of Lampung through GIS processing to generate a vulnerability map based on inundation.

2.5. ALOS AVNIR-2 Image Processing

SAVI was used for mapping vegetation density. Briefly, the digital numbers of ALOS AVNIR-2 were converted to reflectance values before generating the synthetic NDVI and SAVI images [19,20]. A vegetation density map was created as below:

2.5.1. Reflectance Calculation

A radiance conversion from digital number values is required before calculating reflectance. Calculating radiance is a fundamental step in relating image data from multiple sensors and platforms into a common

radiometric scale [21]. The general equation for DN to radiance conversion is demonstrated in equation (3) [22].

$$L_\lambda = G_{rescale} \times QCAL + B_{rescale} \quad (3)$$

where L_λ is spectral radiance at the sensor's aperture (W/m2/sr/μm), Grescale is rescaled gain, $QCAL$ is Digital Number (DN), and $B_{rescale}$ is rescaled bias [23]. Conversion of reflectance is obtained using Equation (4),

$$\rho_\lambda = \frac{\pi \times L_\lambda \times d^2}{ESUN_\lambda \times cos\theta_s} \quad (4)$$

where ρ_λ is unitless planetary reflectance and L_λ is spectral radiance at the sensor's aperture. Meanwhile, $d^2$is the earth-sun distance in astronomical units from a nautical handbook, $ESUN_\lambda$ is mean solar Exoatmospheric irradiances, and θ_s is solar zenith angle in degrees.

2.5.2. NDVI Calculation

The concept of NDVI is about the first channel causing considerable absorption of incoming sunlight and the second channel creating considerable reflectance [24-26]. The differences in wavelength are calculated using NDVI. The range of wavelength used is between -1 and 1, in which 0.5 indicates dense vegetation and < 0 indicates no vegetation, including water [27]. NDVI is calculated as

$$NDVI = \frac{(NIR - VIS)}{(NIR + VIS)} \quad (5)$$

where NIR is Near Infra-Red band, and $VIS$is a visible band of the red band. ALOS AVNIR-2 band 3 is red, and band 4 is NIR.

2.5.3. SAVI Calculation

SAVI can be defined as an algorithm developed to generate vegetation indexes by eliminating soil factor [28]. A SAVI based model is capable of characterising the forested and non-forested area [20]. Therefore, the model is created to reduce soil brightness, such as shadow [29]. NDVI is calculated as [30],

$$SAVI = \frac{(NIR - R)}{(NIR + R + L)} x(1 + L) \quad (6)$$

where NIR is Near Infra-red band, R is red band, and L is the soil calibration factor, in which L is equal to 0.5 [31]. The secondary backscattering effect of canopy transmitted is reduced using a correction factor (L).Lvalue of 1 is optimal in semiarid environments. The SAVI generated map is shown in Figure 7(a).

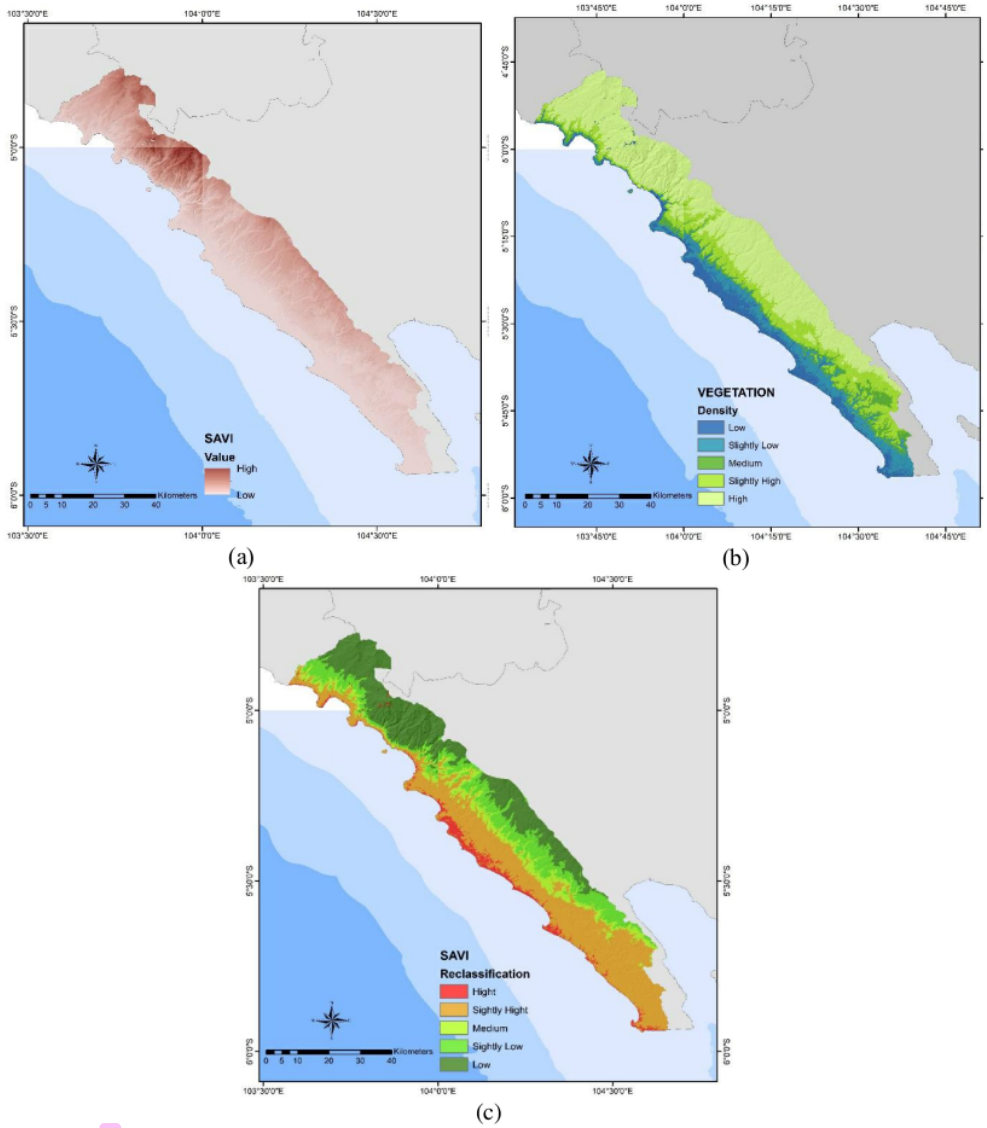

Figure 7. (a) SAVI Map; (b) Vegetation density; and (c) Vulnerability map based on vegetation density

3. Results and discussion

3.1. Tsunami run-up simulation

A scenario simulation was demonstrated in the central earthquake location on the ocean plate of the West coast of Lampung. Tsunami modelling parameters which are length, width, maximum and average displacement were created for measuring time, amplitude, and wave height of the tsunami in one area. The input process of the tsunami model was generated using the bathymetric input data of the earthquake location on the Western region of Sumatera island, and topography data required were used in the ASCII

XYZ format. The results of the input parameters decision for source modelling are shown in Table 2. Subsequently, the mechanism data of earthquake were prepared by deciding on the design modelling, while the grid creation of the bathymetric value, simulation design of tsunami and the wave height of tsunami modelling were then determined. The initial profile of a tsunami centre can be calculated by considering the profile as a seabed deformation with fault parameters which can be determined by using the mechanism solution data of the earthquake centre. Deformations of the seabed as outputs of centre modelling were assessed using tsunami L-2008. Furthermore, it was applied in the ocean and run up modelling. The vertical displacement (deformation of the seabed) as an output of source modelling was needed in the ocean modelling using L-2008 application and bathymetric data. The bathymetric coordinate boundaries of this study were between 4°51'23.43"S to 6°43'50.50"S and 102°3'3.30"E to 105° 2'29.63"E. Moreover, the level of the earthquake was 7.8 SR, and the distance of the coast to the epicentral was 241 km. In this study, the input parameter was observed at 739.66 km x 82.41 km of length and width fault, resulting in a fault area and slip of 60955.38 km^2 and 11.036 m respectively.

Table 2. Earthquake input parameters for source modelling

Parameter		Research Model	
Length (km)	Al1	369.83	369.83
	Al2	369.83	369.83
Width (km)	Aw1	82.41	82.41
	Aw2	0	0
Depth (km)		28	28
Strike (Degree)		312	58
Dip (Degree)		223	64
Slip (m)		11.036	11.036
Mw (Richter)		7.8	7.8
Centre Fault Coordinate	Lat.	-7.082527°	-7.082527°
	Long.	103.307943°	103.307943°
Type Fault		Normal Fault	Normal Fault

The result of the model design was vertical displacement in Figure 8, shown as deformation in the seabed. The movement of deformation which occurred in the seabed was followed by a shift in the sea level. The source modelling results illustrated variation in the maximum vertical displacement and event and a minimum vertical displacement value of 3.35 m and -3.35 m, respectively. The maximum vertical value showed an increase in the seabed vertical movement, but the minimum vertical displacement showed a reduction in the seabed vertical movement. The rapid vertical movement of the seabed was detected as a response to the earthquake and had caused the rise and fall of the sea level. The ocean modelling results showed the propagation of tsunami waves in all directions. In this study, the timing and height that were taken for the propagation of a tsunami wave from the epicentre to the beach (target area) were 28.56 min and 2.65 m, respectively shown in the Figure 9. In this study, the target location was Krui on the west coast Lampung. The run-up modelling result from the calculation fault of the length and width is shown in Figure 10. The run-up score was affected by the distance of the epicentre to the affected area, bathymetric, the morphology of the beach, the slope of the beach, and the wave height of the tsunami [32]. Enhancement of the height of the tsunami wave was comparable with the shallowness of the approaching land.

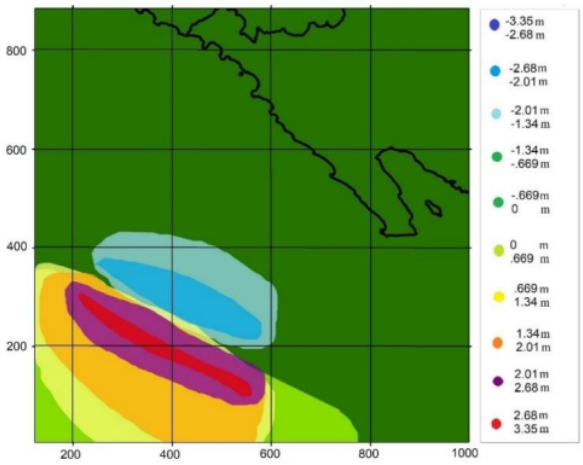

Figure 8. Vertical displacement

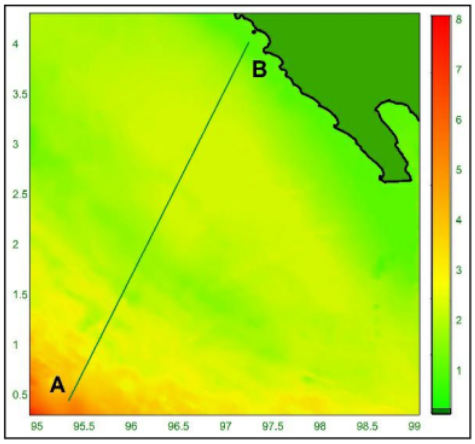

(a)

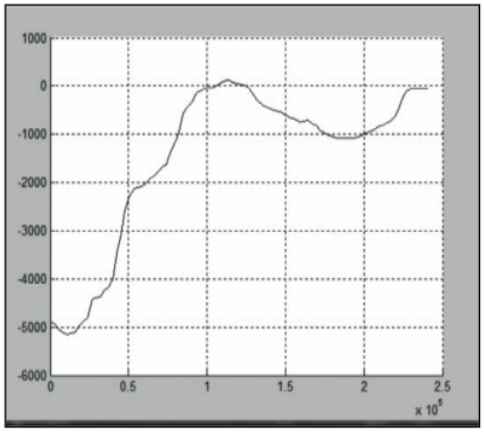

(b)

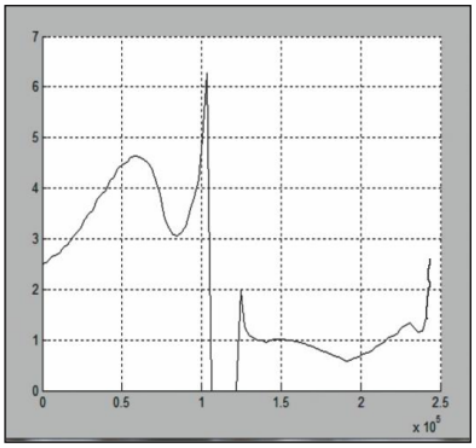

(c)

Figure 9. (a) Cross-section of plot A-B (241 km); (b) Cross-Section of ocean bottom A-B; (c) Cross-section of maximum tsunami height A-B

This phenomenon was followed by refraction, reflection, and diffraction and had brought about a higher tsunami wave. In this study, the height of the run-up and inundation were analysed. The length of the inundation affected the tsunami wave which then affected the population.

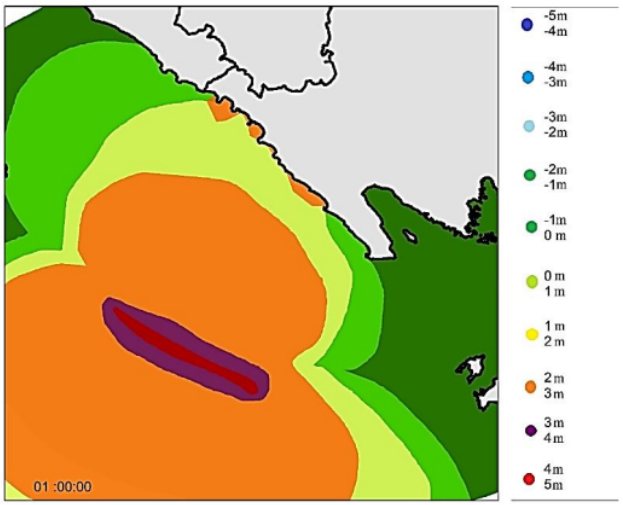

Figure 10. Tsunami height based on calculation

3.2. AHP processing

This study classified all the parameters of tsunami vulnerability into five classes: Number 1, 2, 3, 4, and 5 in which representing low, slightly low, medium, slightly high, and high vulnerability, respectively. All the parameters were assessed using a weighting and scoring system in order to determine the limiting factors of each parameter. The weighting system was also used to determine the different classes of

tsunami vulnerability. The AHP was applied to assess the weight of each parameter using pair-wise comparisons. The AHP method created a scaled set of preferences and described the essential parameters in relation to other parameters [33-37]. In addition, assessed the natural hazards of vulnerability. The sequencing number of 1 to 9 as tabulated in Table 3 was used as a comparison scale to create a pair-wise comparison matrix. The number depended on the relative weight of each parameter and the relative weight was produced by pair-wise comparison in Figure 11.

Table 3: Nine-point comparison scale by Saaty [38]

Intensity of importance	Definition
1	Equal importance
3	Weak importance of one over another
5	Essential or strong importance
7	Demonstrated importance
9	Absolute importance
2,4,6,8	Intermediate value between the two adjacent judgements

Prior to the spatial analysis, a consistency level computation was required. Consistency Ratio (CR)) is a procedure that determines the index of consistency. It shows that the probability of the matrix findings was randomly calculated [35]. In other words, AHP allows inconsistency by using the consistency ratio computation. The tolerable consistency ratio is less than or equal to 10 per cent [39]. CR is the ratio between the consistency index (CI) and random consistency index (RI), and can be expressed using equation (7)

$$CR = \frac{CI}{RI'} \; and \; CI = \frac{(\lambda \, max - N)}{(N-1)} \tag{7}$$

where λmax represents the largest eigenvalue, and N is the size of the comparison matrix. In this study N = 5. λmax was calculated from the sum of all the parameters, and then multiplied by its eigenvector. RI is based on the random consistency index (RI = 1.12 for five parameters). Normalised matrix (Fig. 10) was calculated from the pair-wise comparison in four iterations, and showed that CI was 0.252, while CR was 22.5%. The pair-wise comparison revealed that run-up was the most important factor (50.18%) followed by elevation (19.52%), slope (13.10%), coastline distance (9.53%) and vegetation density (7.67%). AHP results showed that those classes were the most important parameters in deciding vulnerability. Spatial multi-criteria were analysed using the AHP method from which the vulnerability map was created by using weight factors for each parameter. It was found that the run-up parameter showed the highest weight. 0.99% as the data provided in table 4. The area was identified as being slightly high while a high class of tsunami vulnerability was found in the coastal area which has a lower elevation as in Figure 12(b).

Pair-wise comparison matrix

	Elevation	*Slope*	*Coastial Proximity*	*Rund Up*	*Vegetation*
Elevation	1.00	2.00	3.00	0.33	3.00
Slope	0.50	1.00	2.00	0.25	3.00
Coastial Proximity	0.33	0.50	1.00	0.20	3.00
Rund Up	3.03	4.00	5.00	1.00	5.00
Vegetation	0.33	0.33	0.33	0.20	1.00

Normalized Matrix

	Elevation	*Slope*	*Coastial Proximity*	*Rund Up*	*Vegetation*
Elevation	0.1924	0.2553	0.2647	0.1667	0.2000
Slope	0.0962	0.1277	0.1765	0.1263	0.2000
Coastial Proximity	0.0641	0.0638	0.0882	0.1010	0.2000
Rund Up	0.5831	0.5106	0.4412	0.5051	0.3333
Vegetation	0.0641	0.0462	0.0294	0.1010	0.0667

4th iteration

0.1952	0.1952	0.1952	0.1952	0.1952	19.52%
0.1310	0.1310	0.1310	0.1310	0.1310	13.10%
0.0953	0.0953	0.0953	0.0953	0.0953	9.53%
0.5018	0.5018	0.5018	0.5018	0.5018	50.18%
0.0767	0.0767	0.0767	0.0767	0.0767	7.67%

Figure 11. Pair-wise comparison and normalised matrix

3.3. Spatial Analysis for Vulnerability Mapping

The weighted overlay was applied using spatial analysis in GIS after creating a parameter map. In addition, the weighted overlay tool was used to solve multi-criteria problems. The weighted overlay method is a protocol that applies a standard scale of values for various parameters. The overall steps of

this process are shown in the figure 12(a). The level of vulnerability starts from 1 (low vulnerability) to 5 (high vulnerability). Furthermore, the statistic of vulnerability map was calculated. The vulnerability classes as in table 4 were created using the subtraction of maximum and minimum values. Moreover, the number of the class was also used to divide the vulnerability classes. Finally, tsunami vulnerability was mapped into five classes as show by figure 12(b). Results showed that the high vulnerability areas were mostly found in the coastal area with the sloping coast type.

Table 4. Vulnerability classes

Vulnerability Class	Area (square kilometre)	Percentage (%)
High (5)	11.26	0.42%
Slightly High (4)	15.28	0.57%
Medium (3)	266.18	9.93%
Slightly Low (2)	112.218	4.19%
Low (1)	2276.06	84.90%

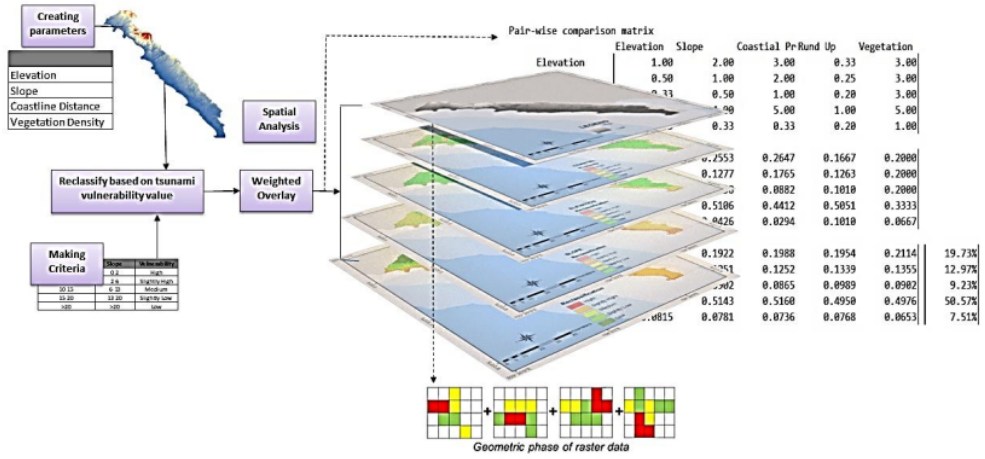

(a)

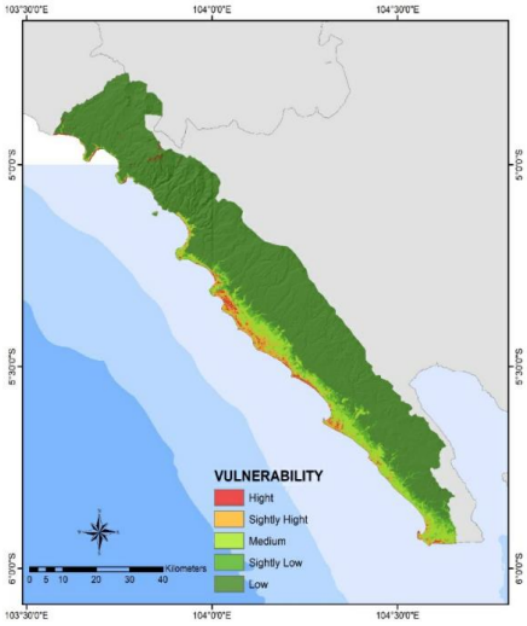

(b)

Figure 12. (a) Spatial analysis step (b) Tsunami vulnerability map of west coast Lampung

3.4. Tsunami inundation and impact assessment

The simulation of tsunami wave results found that the maximum wave height was 2.65 m, inundation area was 26.54 km^2, and vulnerability level was 11.26 km^2. While the building area was estimated at approximately 6.6 km^2 along the West coast of Lampung as in Table 4 and Figure 12, the inundation areas were predicted as high vulnerability and slightly high vulnerability. Meanwhile, a significantly different result of the inundation area (22.09 km^2) was recorded from the previous study [40]. Enhancement of the inundation area in 2019 was 4.45 km^2 compared with the BNPB result in 2016. This might be due to the changing vegetation around the area as vegetation plays an essential role as a tsunami barrier that reduces the impact of tsunami destruction [41-44]. In addition, SAVI values of West coastal Lampung showed the state of vegetation of the inundation area as follows: 6.02 km^2 (22.68%) of low vegetation, 11.85 km^2 (44.65%) of slightly low vegetation and 8.67 km^2 (32.67%) of medium vegetation as in Figure 7 and 12.

Table 5. Vulnerability class of building area

Vulnerability class	Inundation area 5	4	3	2	1
Building area (km^2)	0.91	5.69	3.26	2.69	3.88

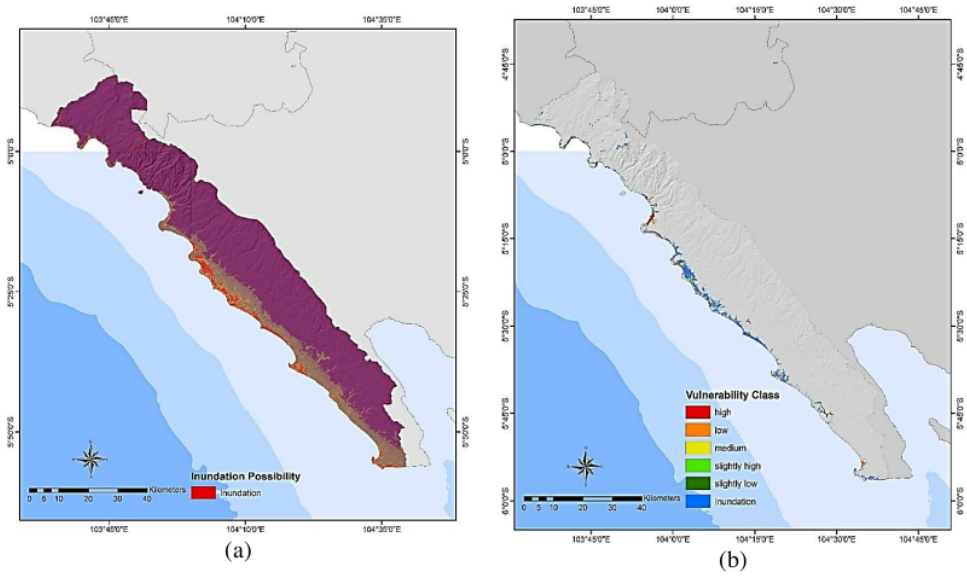

Figure 13. (a) Map of possible inundation area in west coast Lampung (b) Tsunami vulnerability class of building area in west coast Lampung

4. Conclusion

The identification of tsunami vulnerability areas on the west coast of Lampung Province and evaluation of the tsunami impact by mapping possible inundation areas using a geospatial analysis-based tsunami run-up simulation was studied. The simulation was carried out using the L-2008 software. It resulted in a tsunami wave of 2.65 m in height at a timing of 28.56 min when it reached the coast area. There were five parameters that were used to create a tsunami vulnerability map and predict the possibility of an inundation area along the west coast of Lampung, including the run-up, elevation, slope, coastal line, and vegetation. In addition, the analytical hierarchy process (AHP) was used to estimate the weight of the parameters of AHP was calculated using a pair-wise comparison matrix. The results showed *CI* and *CR* values of 0.252 and 22.5%, respectively. The pair-wise comparison revealed that run-up was the most important factor (50.18%) which affected vulnerability and inundation area, followed by elevation (19.52%), slope (13.10%), coastline distance (9.53%) and vegetation density (7.67%). The final map of tsunami vulnerability was constructed using the weighted overlay through a spatial analysis in GIS. Furthermore, the classes of vulnerability were identified into five classes with a series of numbers from 1 (low vulnerability) up to 5 (high vulnerability), and the tsunami inundation mapping was analysed. The assessment result indicates that 11.26 square kilometres of the study area falls under the high vulnerability zone due to tsunami and 6.6 square kilometres of the building area comes under the inundation area. Subsequently, our study has shown that the total number of inundation area along the west coast of Lampung was 26.54 km^2. Therefore, the result of this study can be used as a reference by the local government to facilitate improvements in basic data for city planning related to evacuation processes and management strategies during disasters.

References

[1] Birkmann J 2006 *Measuring Vulnerability to Hazards of Nature Origin* (Tokyo: UNU press) p 1
[2] Birkimann J and Wisner B 2005 *Measuring the Un-Measureable* (Germany:UNU Press) p 40
[3] Papathoma M and Dominey-Howes D 2003 *Nat. Hazard Earth Syst. Sci.***3(6)** 733-747

[4] Papathoma M, Dominey H, Smith D T M and Zong Y 2003 *Nat. Hazard Earth Syst. Sci.***3(5)** 377
[5] Papathoma M and Dominey-Howes D 2003 *Nat. Hazard Earth Syst. Sci.* **3(6)** 734
[6] United Nations Disaster Relief Coordinator (UNDRO) 1991 *Mitigation Natural Disaster: Phenomena, effects and Options, a Manual for Policy Makers and Planners* (United Nations Publication, New York)
[7] Pelling M 2003 *The Vulnerability of cities: Natural Disaster and Social Resilience* (London: Earthscan)
[8] Bollin C, Cardenas C, Hahn H and Vasta K S 2003 *Natural Disaster Network: Disastere Risk Management by Communities and Local Goverment* (Washington DC: Inter American Development Bank)
[9] Schmidt-Thome P 2006 *Natural and Technological Hazards and Risks Affecting the spatial Development of European Regions* (Finland:Special Paper 42 Geological Survey)
[10] Mahendra R S, Mohanty P C, Bisoyi H, Srinivasa K T and Nayak S 2011 *Ocean Coast. Manag.* **54(4)** 302
[11] Caver S J 1991 *Int. J. Geo. Info. Syst.* **5(3)** 321
[12] Jankowski P 1995 *Int. J. Geo. Info. Syst*.**9(3)** 251
[13] Sinaga T P T, Adhi N, Lee Y W and Yongcheol S 2011 *KSCE J. Civ. Eng.* **15(3)** 537
[14] Strunz G, Post J, Zosseder K, Wegsceider S, Muck M, Riedlinger T, Mehl H, Dech S, Birkmann, Gebert N, Harjono H, Anwar H Z, Sumaryono, Khomarudin R M, and Muhari A 2011 *Nat. Hazards Earth Syst. Sci.* **11(1)** 67
[15] Lida K 1963 *Magnitude, Energy and Generation Mechanisms of Tsunami and a Catalogue of Eartquakes Associated with Tsunamis*" (Honolulu:Proceeding of Tsunami Meeting at the 10th Pacific Science Congres) pp 7-18
[16] Van Zuidam R A 1983 *Guide to Geomorphological Aerial Photograpic Interpretation and Mapping* (Enschede:International Institute for Geo Information Science and Eart Observation)
[17] Bretschneider C.L and Wybro P.G 1976 *Coast. Eng. Proc.* **1(5)** 59
[18] Hills J G and Mader C L 2006 *Ann. N. Y. Acad. Sci.* **822(1)** 381
[19] Huete A R 1988 *Rem. Sens. Environ.* **25(3)** 295
[20] Araujo L S, Dos Santos J R and Shimabukuro Y E 2000 *Int. Arch. Photogramm. Remote Sens. Spat. Inf. Sci.* **33** 77
[21] Chander G and Markham B 2003 *IEEE Trasns. Geosci. Remote Sens.***41(11)** 2674
[22] Bouvet M, Chander G, Goryl P and Sater R 2007 *IEEE Int. Geosci. Remote Sens. Symp.* 2673
[23] *Data Users Handbook Data Products, Chapter 11* 2011 (National Aeronautics and Space Administration)
[24] Tucker C J 1979 *Remote Sens. Environt.* **8(2)** 127
[25] Jackson R D, Slater P N and Pinter P J 1983 *Remote Sens. Environ.* **13(3)** 187
[26] Tucker C J, Newcomb W W, Los S O and Prince S D 1991 *Int. J. Remote Sens.***12(6)** 1133
[27] Hansen M C, Defries R S, Townshend J R G and Sohlberg R 2000 *Int. J. Remote Sens.* **21(6-7)** 1331
[28] Gong P, Pu R, Biging G S and Larrieu M R 2003 *IEEE Trans. Geosci. Remote Sens.* **41(6)** 1355
[29] Huete A R, Hua G, Qi J, Checbouni A and Van Leeuwen W J D 1992 *Remote Sens. Environ.* **41(2-3)** 143
[30] Huete A R 1988 *Remote Sens. Environ.* **25(3)** 295
[31] Jensen J R 2000 *Remote Sensing of the Environment An Earth Resource Perspective* (Prentice Hall, Upper Sadle River)
[32] *Peta Sumber Bahaya Gempa Indonesia* 2017
[33] Rahmawati N I, Santosa B J, Setyonegoro W, Bambang S 2017 *Jurnal Sains dan Seni* **6(20)** 2337
[34] Latief, H., Sunendar H, Yuhsananta. P and Riawan E 2006 *Laporan Program Penelitian dan Pengembangan IPTEK* **155**
[35] Saaty T L 1970 *J. Math Psyc.***15(3)** 234
[36] Saaty T L 1980 *The Analytic Hierarchy Process, Planning,Priority Setting, Resource Allocation*

(New York:McGraw Hill)
[37] Saaty T L 2003 *Eur. J. Oper. Res.* **145(1)** 85
[38] Forman E H and Selly M A 2001 *Decision by Objectives* (World Scientific Publishing Company)
[39] Saaty T L 1996 *Decision Making for Leaders: The Analytical Hierarchy Process for Decisions in a Complex World* (Pittsburgh:RWS Publications)
[40] Harada K, Imamura F 2002 *Proc. 12th Int. Offshore Polar Eng. Kitakyushu* pp 652-658
[41] Alongi D M 2008 *Estuar. Coast. Shelf Sci J.* **76(1)** 1
[42] Pranata Y A dan Johnny G P 2014 *Jurnal Teknik Sipil* **13(1)** 25
[43] Husrin S, Jaya K, Aprizon P, Joko P, Yudhi C, Aditya H 2015 *Procedia Earth and Planetary Science* **12(2005)** 20
[44] Susanto D, Faida L R and Sunarto S 2019 *Jurnal Ilmu Kehutanan* **13(1)** 4

Vulnerability Assessment of Tsunami-Affected Inundated Area Using Geospatial Analysis Based Tsunami Run-Up Simulation

ORIGINALITY REPORT

19%	15%	18%	5%
SIMILARITY INDEX	INTERNET SOURCES	PUBLICATIONS	STUDENT PAPERS

PRIMARY SOURCES

1	Rina Febrina, D K Evan, Lusmeilia Afriani, Rr M I Retno, Susilorini, Helmia Adita Fitra. "The analysis of Tsunami evacuation route based on geographic information system: a case study in the coast of Lampung Bay", IOP Conference Series: Materials Science and Engineering, 2020 Publication	6%
2	file.scirp.org Internet Source	5%
3	repositary.knuba.edu.ua:8080 Internet Source	4%
4	Abu Bakar Sambah, Fusanori Miura. "Integration of Spatial Analysis for Tsunami Inundation and Impact Assessment", Journal of Geographic Information System, 2014 Publication	1%
5	petit.lib.yamaguchi-u.ac.jp Internet Source	1%

6	centaur.reading.ac.uk Internet Source	1 %
7	www.intechopen.com Internet Source	1 %

Exclude quotes	On	Exclude matches	< 1%
Exclude bibliography	On		

Vulnerability Assessment of Tsunami-Affected Inundated Area Using Geospatial Analysis Based Tsunami Run-Up Simulation

GRADEMARK REPORT

FINAL GRADE

/0

GENERAL COMMENTS

Instructor

PAGE 1

PAGE 2

PAGE 3

PAGE 4

PAGE 5

PAGE 6

PAGE 7

PAGE 8

PAGE 9

PAGE 10

PAGE 11

PAGE 12

PAGE 13

PAGE 14

PAGE 15

PAGE 16

PAGE 17

PAGE 18

PAGE 19